Spin Dependence in Polarized $p\ p \to p\ p$ and $p\ C \to p\ C$ Elastic Scattering at Very Low Momentum Transfer t at RHIC

A. Bravar[a], I. Alekseev[b], G. Bunce[ac], S. Dhawan[d], R. Gill[a], H. Huang[a], W. Haeberli[e], G. Igo[f], O. Jinnouchi[c], A. Khodinov[g], A. Kponou[a], K. Kurita[h], Y. Makdisi[a], W. Meng[a], A. Nass[a], H. Okada[i], N. Saito[ic], H. Spinka[j], E. Stephenson[k], D. Svirida[b], D. Underwood[j], C. Whitten[f], T. Wise[e], J. Wood[f], and A. Zelenski[a]

[a]Brookhaven National Laboratory, Upton, NY 11973, USA

[b]ITEP, Moscow, 117259, Russia

[c]RIKEN BNL Research Center, Upton, NY 11973, USA

[d]Yale University, New Haven, CT 06511, USA

[e]University of Wisconsin, Madison, WI 53706, USA

[f]UCLA, Los Angeles, CA 90095, USA

[g]SUNY at Stony Brook, Stony Brook, NY 11794 USA

[h]Rikkyo University, Toshima-ku, Tokyo 171-8501, Japan

[i]Kyoto University, Sakyo-ku, Kyoto 606-8502, Japan

[j]Argonne National Laboratory, Argonne, IL 60439, USA

[k]Indiana University, Bloomington, IN 47405, USA

Interference phenomena in (polarized) hadron collisions have often led to spectacular spin effects in the final state. These effects are expressed in terms of the spin observables, like the Analyzing Power A_N. The interference of the electromagnetic spin-flip amplitude with a hadronic spin-nonflip amplitude in the elastic scattering of hadrons generates a significant A_N at very low t ($0.001 < |t| < 0.01$ (GeV/c)^2). This kinematical region is referred to as the Coulomb Nuclear Interference (CNI) region. A possible hadronic spin-flip amplitude can substantially modify the magnitude and shape of A_N, which otherwise is exactly calculable. First results on A_N in polarized proton–proton elastic scattering in the CNI region at 100 GeV from the 2004 polarized proton run at RHIC are presented. New results on A_N in the elastic scattering of polarized protons off a carbon target over a wide energy range from 4 GeV to 100 GeV from AGS and RHIC are presented, as well. These results allow us to further study the spin dependence in elastic scattering and the mechanisms that generate these effects.

In some sense elastic scattering of hadrons is the simplest and the most basic type of nuclear interaction (see Figure 1), yet elastic scattering phenomena have eluded a detailed and satisfactory explanation from general principles for a long time. When studying unpolarized reactions, we average over all initial polarization states and sum over all final states, thus losing important information on the interaction dynamics and forces, which are spin dependent. The formalism for polarized elastic scattering is well developed in terms of five independent helicity amplitudes $\phi_i(t)$ [1] with, however, little understanding of the mechanisms at work. The region of low 4-

momentum transfer t is associated with long distance phenomena, and therefore is in the domain of non-perturbative QCD, where no precise calculations can be made. Several meson exchange models based on Regge phenomenology have been developed to describe the observed data. Naively one would expect that simple concepts like angular momentum conservation and helicity conservation in the $s-$channel lead to simple and predictable spin effects in elastic scattering. Most of these models, that otherwise seemed to work, failed to predict the observed spin dependencies.

With internal targets (atomic hydrogen jet target and carbon ribbons) the RHIC accelerator can be operated also in a fixed target mode, with typical energies of $\sqrt{s} = 7 - 22$ GeV. In this talk I will discuss recent A_N results in pp and pC elastic scattering in the very low t region of $|t| <$ few $\times 10^{-2}$(GeV/c)^2 from the 2004 polarized proton run at RHIC using internal targets.

The analyzing power A_N is a measure of the left–right asymmetry of the cross section in the scattering plane normal to the beam or target polarization. A_N arises from the interference between a spin-flip and spin-nonflip amplitude and thus provides basic information on the spin dependence of the interaction. In terms of helicity amplitudes $\phi_i(t)$, A_N is expressed as:

$$A_N \frac{\mathrm{d}\sigma}{\mathrm{d}t} = -\mathrm{Im}\left[\phi_5^* \left(\phi_1 + \phi_2 + \phi_3 - \phi_4\right)\right] , \qquad (1)$$

where $\frac{\mathrm{d}\sigma}{\mathrm{d}t}$ is the spin averaged cross section and ϕ_5 is the single spin-flip helicity amplitude.

In high energy pp and pA elastic scattering at very low 4-momentum transfer t, A_N originates from the interference between the electromagnetic (Coulomb) spin-flip amplitude, which is generated by the proton's anomalous magnetic moment, and the hadronic (Nuclear) spin-nonflip amplitude (CNI = Coulomb Nuclear Interference) [2]. These two amplitudes are almost orthogonal to each other in the complex plane, with the electromagnetic amplitude being real. A_N reaches a predicted maximum value of about 4–5 % around a t value of 3×10^{-3} (GeV/c)^2 and decreases with increasing $|t|$ [2].

The existence of a potential hadronic spin-flip amplitude interfering with the electromagnetic spin-nonflip amplitude introduces a deviation in shape and magnitude for A_N calculated with no hadronic spin-flip. [3]. While the former contribution is fully calculable, the latter can be tackled only in Regge inspired phenomenological approaches [3,4]. Note that the conservation of angular momentum imposes restrictions on the helicity-flip amplitudes in the forward direction (i.e. for $|t| \to 0$) and $\phi_5(t) \propto \sqrt{|t|}$. The hadronic spin-flip amplitude carries important information on the static properties and on the constituent quark structure of the nucleon, since the $|t|$ dependence of this hadronic spin-flip amplitude at small $|t|$ is tightly connected with the structure of hadrons.

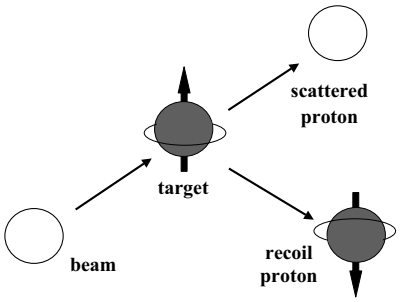

Figure 1. The elastic scattering process: sometime the recoil proton flips its spin yielding to the left–right scattering asymmetry, A_N.

Within Regge phenomenology, one can probe the long standing issue of the magnitude of the Pomeron spin-flip through the study of A_N in the CNI region. In a quark-diquark picture of the proton the magnitude of the Pomeron spin-flip amplitude can be associated with the diquark separation, the smaller this separation the bigger the effect, suggesting thus that the spin part of the Pomeron probes the smallest distances in the proton.

The main motiviation for studying polarized elastic scattering in the CNI region, however, comes from a need of very precise beam polarization measurements at RHIC [5] for the detailed study, for instance, of the nucleon spin structure [6].

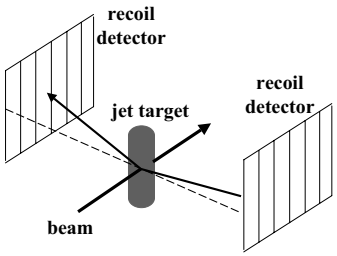

Figure 2. Layout of the pp elastic scattering setup. The atomic beam crosses the RHIC beam from the above.

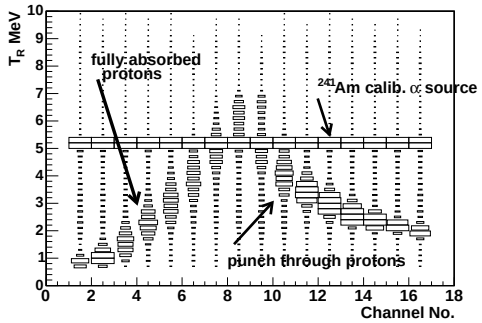

Figure 3. T_R vs. ϑ_R correlation: ϑ_R is measured by the detector channel number in 0.5 mrad steps. The locus on the left is generated by protons fully absorbed, while the locus on the right is due to punch through protons, which deposit only a fraction of their energy in the recoil detectors.

$p\ p^{\uparrow} \rightarrow\ p\ p$

Figure 2 shows the schematic layout of the pp elastic scattering experiment. In the CNI region recoil protons from pp elastic scattering emerge close to 90° with respect to the beam direction. The recoil protons were detected using an array of silicon detectors located at ~ 80 cm from the jet target axis on both sides of the beam and covered an aziumuthal angle of $\sim 15°$ on each side. Each array consisted of 3 silicon detectors segmented horizontally, 80×50 mm^2 in size, with a ~ 4.4 mm readout pitch. These detectors provided energy ($\Delta T_R \leq 60$ keV), polar angle ($\Delta\vartheta_R \sim 1.6$ mrad) and time of flight (ΔToF ~ 3 ns, from intrinsic resolution and bunch length) measurements of the recoil particles. The scattered beam proton does not exit the beam pipe and it is not detected in this experiment. In the covered t region, however, the elastic process is fully constrained by the recoil particle only, thus the detection of the scattered beam proton is not mandatory.

Recoil protons were identified on the basis of the ToF – T_R non-relativistic relation $T_R = \frac{1}{2}M_p(\mathrm{dist/ToF})^2$ and selected on the basis of the $\vartheta_R - T_R$ relation $T_R \simeq 2M_p\vartheta_R^2$, shown in Figure 3. In the t range of $0.001 < |t| < 0.01$ (GeV/c)^2 the recoil protons were fully absorbed in the recoil detectors. On the basis of the ϑ_R – T_R correlation one can reconstruct the mass of the scattered particle (so called missing mass M_X). For a pp elastic scattering process $M_X = M_p$. We found that $M_X \simeq M_p$ with little background below the elastic peak (Figure not shown), confirming indeed that we were selecting pp elastic scattering events. The estimated background in the selected pp elastic scattering sample was less than 5%.

The polarized hydrogen gas jet target crossed the RHIC beams from the above with its polarization directed vertically. The polarized target is a free atomic beam jet. The state-of-art atomic polarized source delivered polarized protons with a polarization of 0.924 ± 0.018 (the dilution from molecular hydrogen is included in this figure), a density in excess of 10^{12} p/cm^2 in its center, and a FWHM profile of less than 6 mm. The target polarization was reversed each 5 to 10 minutes, thus cancelling most of systematic effects associated with the asymmetry extraction. The target polarization was constantly monitored with a Breit-Rabi polarimeter. For more details on the jet target see, for instance, Ref. [7].

Figure 5 shows the analyzing power $A_N(t)$ for pp elastic scattering in the t range of $0.001 < |t| < 0.01$ (GeV/c)^2 at $\sqrt{s} \simeq 14$ GeV. The displayed errors are statistical only. The two major sources of systematic errors come from the backgrounds and the error on the target polarization: the former is estimated around $\delta A_N^{sys} = 0.0015$ for each measured data point and the latter represents a

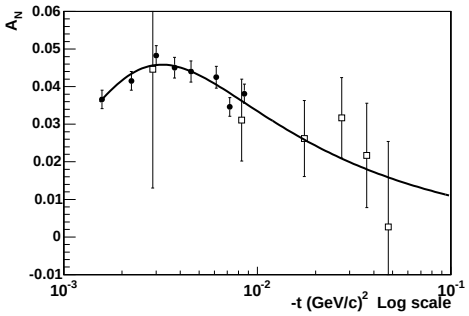

Figure 4. $A_N(t)$ in pp elastic scattering; filled circles: this experiment, open squares: E704 at Fermilab [8]. The errors shown are statistical only. For details on the systematic errors see text. The solid line is the CNI – QED prediction with no hadronic spin-flip.

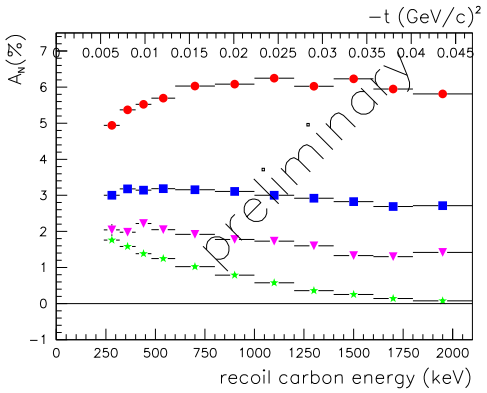

Figure 5. A_N in % for $pC \to pC$ as function of T_R at 4 different beam energies: starting from top E_B = 3.9 GeV, 6.5 GeV, 9.7 GeV, and 21.7 GeV. The displayed errors are statistical only.

normalization uncertainty of 2.0%. These data are also compared to a previous, much less precise measurement from the Fermilab E704 experiment at $\sqrt{s} \simeq 20$ GeV [8].

These data are well described by the CNI prediction with no hadronic spin-flip terms ϕ_5^{had} [3]. In Figure 5 the A_N data are fitted with the CNI prediction with a free normalization factor N: $\chi^2/\text{d.o.f.} \simeq 5/7$ with $N = 0.98 \pm 0.03$. The interpretation, therefore, does not require additional hadronic spin-flip terms; the sensitivity on ϕ_5^{had} in this t region, however, is limited. A_N data in the larger t range of $0.01 < |t| < 0.03$ (GeV/c)^2 will soon become available. Data on the double spin asymmetry A_{NN} in the same t range will be soon available, as well. That will allow us to perform more extensive studies of the spin dependence in pp elastic scattering and of the mechanisms at work, and draw firmer conclusions on ϕ_5^{had}.

$p^{\uparrow}C \ \to \ p \ C$

A setup similar to the one shown in Figure 2 is used for the pC elastic scattering measurements. A carbon ribbon target, as thin as 3.5 μg/cm^2, is inserted from time to time into the AGS and RHIC polarized proton beams. pC elastic scattering events are identified on the basis of the ToF – T_R correlation for the recoil carbon ions.

Figure 5 shows the A_N results for pC elastic scattering as a function of the recoil carbon energy T_R ($T_R = |t|/2M_C$) at several incident beam energies E_B from 4 to 22 GeV using the AGS polarized proton beam. At beam energies below 10 GeV a very weak $|t|$ dependence and much larger asymmetries are observed compared to the CNI-type behavior at larger energies. The normalization uncertainty is $\sim$ 10% for the lowest energy data points and increases to $\sim$ 20% for the highest ones. The systematic error, which comes mainly from backgrounds below the elastic pC peak, pileup and electronic noise, is estimated to be $<$ 15% relative. In Figure 6 the same A_N data are shown as a function of E_B for different t intervals. At larger values of E_B there appears to be a weak or no energy dependence; this behavior is suggestive of the onset of an asymptotic regime.

Figure 7 shows the A_N data as a function of t for pC elastic scattering at 100 GeV using the RHIC polarized proton beam over a wide t interval. For this measurement $P_B = 0.386 \pm 0.033$ as measured with the jet target. The systematic errors, displayed as a band in Figure 7,

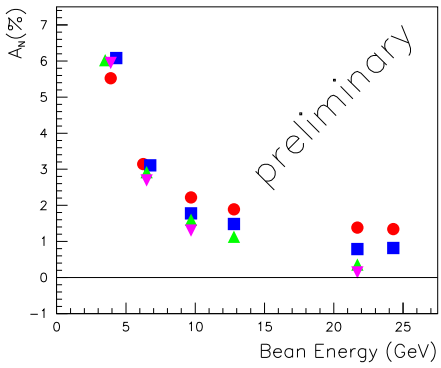

Figure 6. A_N as a function of E_B for different intervals of t: full circles $|t| \sim 0.01$ GeV$^2/c^2$, squares $|t| \sim 0.02$ GeV$^2/c^2$, up triangles $|t| \sim 0.03$ GeV$^2/c^2$, down triangles $|t| \sim 0.04$ GeV$^2/c^2$.

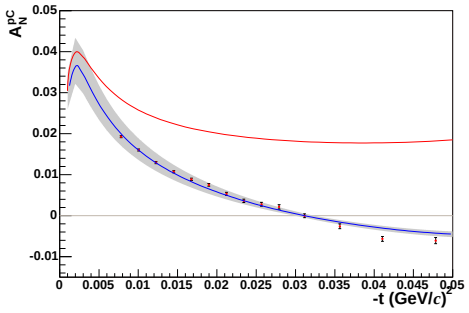

Figure 7. $A_N(t)$ for pC elastic scattering at 100 GeV. The shaded band represents the systematic uncertainties of the measurement. The solid line in the band is a fit to the data including a significant hadronic spin-flip contriubtion (see text). The result is significantly different from the no hadronic spin-flip prediction (top curve).

come mainly from the normalization uncertainty $\Delta P_B/P_B \sim 8.5\%$ and the energy scale in determining the recoil carbon energy T_R. The systematic errors on the raw asymmetry measurement alone, however, are very small.

In Figure 7 these data are fitted with a phenomenological model developed in Ref. [4], which introduces a hadronic spin-flip contribution to A_N via the ω, f_2, and Pomeron trajectories. Contrary to the pp elastic scattering case, these data require a significant hadronic spin-flip contribution. The r_5 value from the best fit is Re $r_5 = 0.051 \pm 0.002$ and Im $r_5 = -0.012 \pm 0.009$. The uncertainty is mainly due to the two systematic error sources described above. Im r_5 and Re r_5 are strongly anti-correlateed and the 1-σ contour for (Re r_5, Im r_5) ranges from (0.070, -0.16) to (0.035, 0.110). Note that a small amplitude (here the spin-flip one) can generate large effects, as those shown in Figure 7, through the interference with a large amplitude (the spin-nonflip one).

Comprehensive studies and modeling of A_N over the whole energy range should allow us to better understand and disentangle the various contributions to A_N, the role of the hadronic spin-flip amplitudes, and the possible onset of asymptotic regimes.

We would like to thank the Instrumentation Division at BNL for their work on the silicon detectors and electronics and W. Lozowski at IUCF for providing the carbon ribbon targets. This work is performed under the auspices of U.S. DOE contract Nos. DE-AC02-98CH10886 and W-31-109-ENG-38, DOE grant No. DE-FG02-88ER40438, NSF grant PHY-0100348, and with support from RIKEN, Japan.

REFERENCES

1. M. Jacob and G.C. Wick, Ann. Phys. **7**, 404 (1959).
2. B.Z. Kopeliovich and L.I. Lapidus, Sov. J. Nucl. Phys. **19**, 114 (1974).
3. N.H. Buttimore *et al.*, Phys. Rev. D **59**, 114010 (1999).
4. B.Z. Kopeliovich and T.L. Trueman, Phys. Rev. D **64**, 034044 (2001).
5. A. Bravar *et al.*, AIP Conf. Proc **675**, 830 (2003)
6. G. Bunce *et al.*, Annu. Rev. Nucl. Part. Sci. **50**, 525 (2000).
7. A. Zelenski *et al.*, AIP Conf. Proc **675**, xxx (2003).
8. N. Akchurin *et al.*, Phys Rev. D **48**, 3026 (1993).